UDK 669.24:537.226.86:620.178.3
Original scientific article/Izvirni znanstveni članek

ISSN 1580-2949
MTAEC9, 58(5)567(2024)

EFFECTS OF TEMPERATURE AND STRAIN AMPLITUDE ON LOW-CYCLE FATIGUE PROPERTIES OF NICKEL-BASED SINGLE-CRYSTAL SUPERALLOY DD419

VPLIV TEMPERATURE IN AMPLITUDE DEFORMACIJE NA LASTNOSTI MALO-CIKLIČNEGA UTRUJANJA MONO-KRISTALINIČNE SUPER ZLITINE NA OSNOVI NIKLJA VRSTE DD419

Xiaoming Du[1*], Weiye Dong[1], Xiang Zhu[1], Jide Liu[2], Zhijun Wang[3], Tianfu Li[3]

[1]School of Materials Science and Engineering, Shenyang Ligong University, Shenyang 110159, People's Republic of China
[2]Institute of Metal Research, Chinese Academy of Sciences, Shenyang 110016, People's Republic of China
[3]China Institute of Atomic Energy, Beijing 102413, People's Republic of China

Prejem rokopisa – received: 2024-04-25; sprejem za objavo – accepted for publication: 2024-08-20

doi:10.17222/mit.2024.1169

High-temperature and low-cycle fatigue tests were conducted on a nickel-based single-crystal superalloy DD419 under total strain-controlled conditions at 760 °C and 980 °C. The fatigue properties of the alloy are discussed by analysing the fatigue test data. Fracture morphology and dislocation structure were observed using scanning electron microscopy and transmission electron microscopy. At the same strain amplitude, the results indicate that the plastic deformation of the alloy is larger at 980 °C compared to 760 °C. This leads to a lower fatigue strength and shorter fatigue life, along with more severe damage. The value of the strain amplitude affects the cyclic stress response behaviour of the alloy. Under low strain amplitudes, the cyclic stress response behaviour differs between 760 °C and 980 °C. The hysteresis loop exhibits similar shapes at 760 °C and 980 °C, with an increase in the area as the strain amplitude rises. The fatigue fracture analysis indicates that micropores on the surface are the primary fatigue sources at 760 °C, while oxides on the surface are the main fatigue source at 980 °C, leading to cracking due to multiple sources. Moreover, transmission electron microscopy reveals that the deformation mechanism involving dislocations at 760 °C primarily occurs through plane slip and wave slip, whereas at 980 °C, dislocations mainly move through cross slip and climb.

Keywords: nickel-based single-crystal superalloy, low-cycle fatigue, temperature, strain

Avtorji v članku opisujejo visoko-temperaturne teste malo-cikličnega utrujanja preizkušancev iz Ni monokristalinične superzlitine vrste DD419 v pogojih popolne deformacije pri 760 °C in 980 °C. Avtorji v članku opisujejo trajno dinamične lastnosti izbrane zlitine na osnovi dobljenih rezultatov preizkusov. Morfologije prelomov preizkušancev so avtorji članka opazovali s pomočjo vrstične in presevne elektronske mikroskopije (SEM in TEM). Pri enaki amplitudi deformacije so rezultati preizkusov pokazali, da je plastična deformacija preizkušancev večja pri 980 °C kot tista dobljena pri 760 °C. To posledično vodi do nižje trajne trdnosti, krajše življenske dobe izbrane zlitine in k njenim bolj nenadnim porušitvam. Vrednosti deformacijske amplitude vplivajo na ciklični napetostni odgovor izbrane zlitine. V pogojih nizkih deformacijskih amplitud se ciklična napetostna odgovora pri 980 °C in pri 760 °C razlikujeta med seboj. Oblika histerezne zanke je približno enake oblike pri obeh temperaturah in z naraščanjem amlitude se povečuje njen presek. Na trajnostnih prelomih preizkušancev testiranih pri 760 °C so na površini mikro pore, kar je tudi primarni vzrok za utrujanje materiala. Na preizkušancih testiranih pri 980 °C pa je primarni vzrok za odpoved materiala zaradi utrujanja prisotnost oksidnih vključkov. Nadalje avtorji ugotavljajo na osnovi TEM preiskav, da mehanizem deformacije pri 760 °C primarno poteka z drsenjem dislokacij po drsnih ravninah in s pomočjo valovitega drsenja. Pri 980 °C pa deformacija poteka s pomočjo prečnega drsenja in plezanja dislokacij.

Ključne besede: mono-kristalinična superzlitina na osnovi Ni, malociklično utrujanje, temperatura, deformacija

1 INTRODUCTION

Nickel-based single-crystal (SX) superalloys have become essential materials for hot-end components, especially turbine blades, because of their superior mechanical properties.[1–3] Turbine blades are subjected to substantial thermal stress, as well as high-temperature conditions characterized by intense centrifugal forces and asymmetric alternating loads during an actual operation.

Low-cycle fatigue (LCF) damage is the primary cause of the blade material failure. Consequently, it is necessary to consider the LCF behaviour of SX superalloys. Extensive studies have been conducted on the effects of cyclic frequency, strain rate, strain range, holding period, predeformation, corrosive environment, and testing temperature on high-temperature LCF.[4–7] Fan et al. conducted a study on the impact of temperature and strain amplitude on the fatigue life of the DD10 alloy. The findings indicate that the LCF life of the DD10 alloy is influenced by temperature. In the low strain range, the LCF life at 760 °C surpasses that at 980 °C, while in the high strain range, the opposite trend is observed. The formation mechanism of fatigue fractures in the DD10 alloy varies with temperature.[8] Ding et al. investigated the deformation mechanism of an SX superalloy at different

*Corresponding author's e-mail:
du511@163.com (Xiaoming Du)

temperatures. They provided a detailed analysis of the effects of microscopic dislocation motion in three temperature ranges ($T \leq 750$ °C, 850 °C $\leq T \leq$ 900 °C, and $T \geq 1000$ °C) on the properties and deformation behaviour of the alloy.[9]

At present, the DD419 alloy has been shown to exhibit exceptional mechanical properties at high temperatures. However, there have been few studies on the effects of various temperatures and strain ranges on the LCF properties of the alloy. Therefore, this paper investigates the relationships between temperature, strain amplitude, and LCF properties of the DD419 alloy. The purpose of this study is to comprehensively understand the effect of temperature on the LCF behaviour, fatigue fracture characteristics, and dislocation morphology of DD419 alloy. In this paper, the results can provide valuable references for a practical application of single-crystal superalloys in the engineering field.

2 EXPERIMENTAL PART

The experimental alloy used in this work is a second-generation SX superalloy, DD419, which contains 6.8 % Cr, 9.3 % Co, 6.5 % W, 1.0 % Mo, 3.0 % Re, 5.8 % Al, 1.1 % Ti, 6.5 % Ta, 0.09 % Hf, and Ni in balance (by weight). A single-crystal superalloy billet (purchased) was fabricated using a vacuum induction furnace with the high-rate solidification (HRS) technique.

The single-crystal superalloy billet underwent the standard heat treatment, which included a solution treatment at 1300 °C for 9 h in air, and a two-step aging treatment. The first step involved aging at 1150 °C for 4 h, followed by the second step at 870 °C for 14 h, with both steps being followed by air-cooling. LCF samples were cut from the billet using an electric discharge machine and then machined into LCF specimens with a diameter of 6 mm and a gauge length of 72 mm.

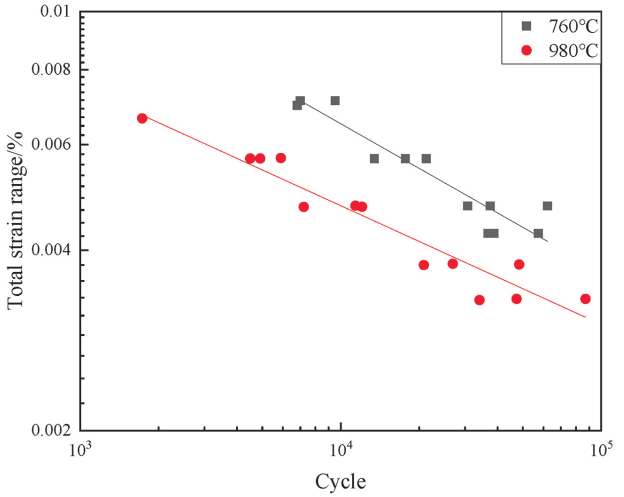

Figure 1: Relation curves for fatigue life and total strain amplitude at different temperatures

The specimens with a diameter of 6 mm were used for the LCF tests. The orientation of the test bar deviating from [001] was within 8°, as determined by the X-ray backscattering Laue method. A servo-hydraulic testing machine was used to conduct fatigue tests at 760 °C and 980 °C with a total strain amplitude of 1.4 %. The constant strain control loading mode was employed, utilizing a triangular waveform. The strain rate was 0.006 s^{-1}, and the strain ratio was $R = 0.05$. The temperature fluctuation over the gauge length was maintained within ±2 °C; all the tests were performed in air. After conducting the LCF tests, the fracture surfaces were examined using a scanning electron microscope (SEM) (TESCAN Maia3). The dislocation was observed using a transmission electron microscope (TEM) (Tecnai G2 F30) operating at an acceleration voltage of 120 kV.

3 RESULTS AND DISCUSSION

3.1 LCF life

Figure 1 illustrates the relationship between the total strain amplitude and the fatigue life of the alloy at the two temperatures. At both temperatures, the life decreases with an increase in strain amplitude. The slope of $\Delta\varepsilon_t/2 - 2N_f$ curve at 760 °C is greater than that at 980 °C, indicating that N_f is more sensitive to a strain variation at 760 °C. In other words, the influence of temperature on the fatigue life becomes more significant with higher strain amplitudes.

The total strain amplitude in LCF testing under a strain control can be expressed as the sum of the elastic and plastic strain amplitudes, as expressed with the Manson-Coffin equation below:[0]

$$\frac{\Delta\varepsilon_t}{2} = \frac{\Delta\varepsilon_e}{2} + \frac{\Delta\varepsilon_p}{2} = \frac{\sigma_f'}{E}(2N_f)^b + \varepsilon_f'(2N_f)^c \quad (1)$$

where $\Delta\varepsilon_t/2$, $\Delta\varepsilon_e/2$ and $\Delta\varepsilon_p/2$ represent the total strain amplitude, the elastic strain amplitude, and the plastic strain amplitude, respectively. N_f is the number of cycles to failure; σ_f' and ε_f' are the fatigue strength and ductility coefficient, respectively; b and c are the material's constants for the selected alloy; and E is Young's modulus.

Figure 2 shows the fitting curves for $\Delta\varepsilon_e/2 - 2N_f$ and $\Delta\varepsilon_p/2 - 2N_f$ for the alloy at 760 °C and 980 °C. The fitted fatigue parameters are listed in **Table 1**. The specific form of the Manson-Coffin equation at 760 °C and 980 °C is as follows:

$$\frac{\Delta\varepsilon_t}{2} = 0.0570(2N_f)^{-0.2388} + 0.0571(2N_f)^{-0.3899} \quad (2)$$

$$\frac{\Delta\varepsilon_t}{2} = 0.0233(2N_f)^{-0.1784} + 0.0589(2N_f)^{-0.6173} \quad (3)$$

It can be seen from **Figure 2** that at all testing strain levels, the values of the plastic strain amplitude for alloy DD419 are much smaller than the elastic strain amplitude at both temperatures, being similar to most SX superalloys.[10–12] As $\Delta\varepsilon_e/2 - 2N_f$ and $\Delta\varepsilon_p/2 - 2N_f$ have no

intersection points, there is no transition fatigue life (N_{tf}) where $\Delta\varepsilon_e/2 = \Delta\varepsilon_p/2$.[13] The references suggest that elastic strain plays a dominant role in the fatigue failure of the alloy,[8] and that there is a strong correlation with fatigue life.

Table 1: Fatigue parameters of DD419 at different temperatures

Temperature (°C)	σ_f' (MPa)	ε_f'	b	c	E (GPa)
980 °C	2049	0.0589	–0.1784	–0.6173	88
760 °C	6180	0.0051	–0.2388	–0.3899	108

In **Table 1**, it is demonstrated that σ_f' decreases with increasing temperature. This implies that as the temperature increases, the fatigue strength of the alloy decreases, leading to a shorter fatigue life. In short, this is consistent with the relationship between the total strain amplitude and fatigue life of the alloy shown in **Figure 1**.

3.2 Cyclic stress response behaviour

Figure 3 presents the cyclic stress response behaviour for DD419 tested at 760 °C and 980 °C at various

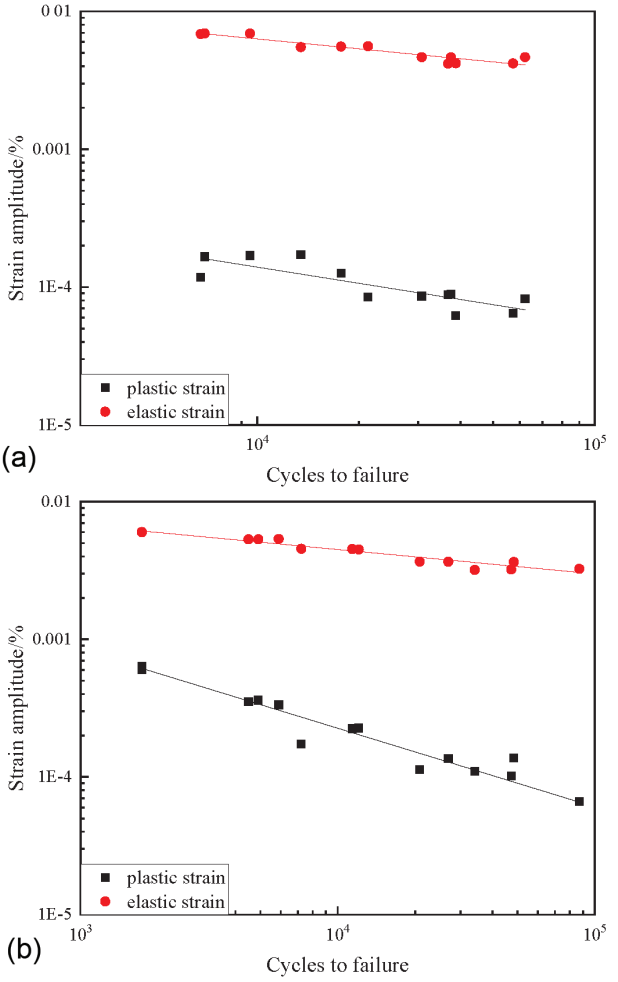

Figure 2: Strain amplitude versus the number of failure cycles at different temperatures: a) 760 °C, b) 980 °C

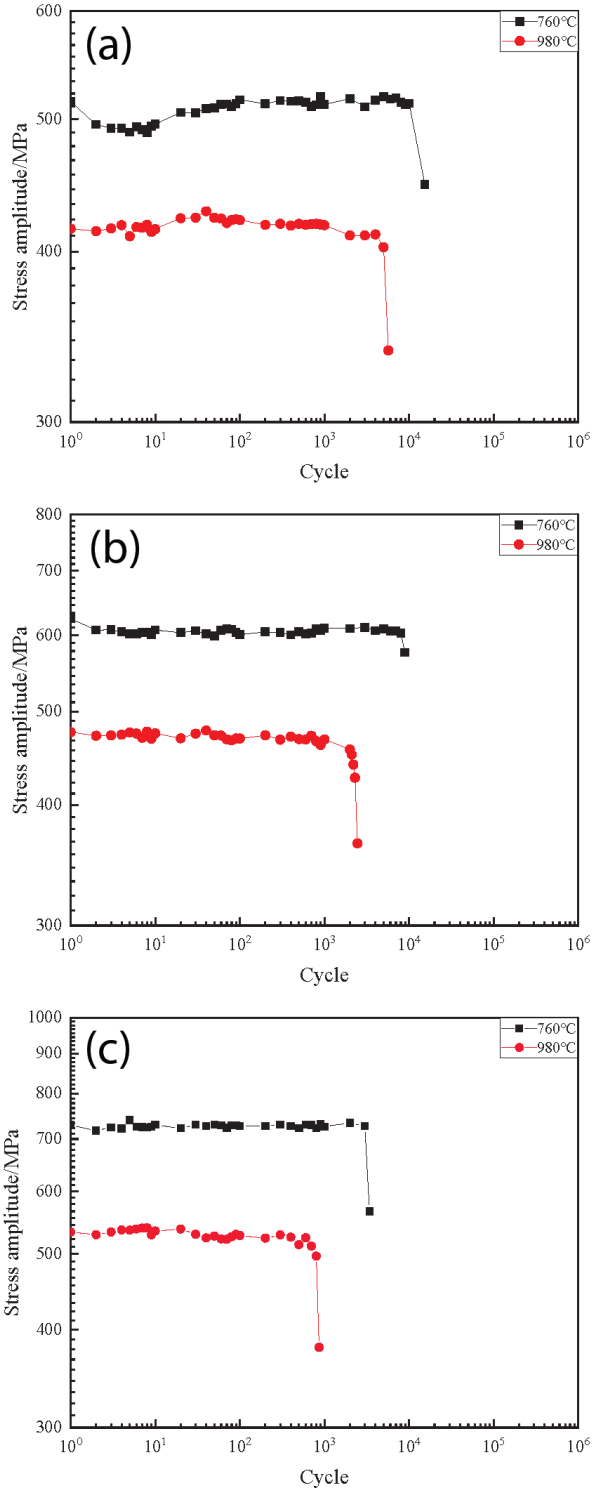

Figure 3: Cyclic stress response curves for three different strain amplitude fatigue tests at 760 °C and 980 °C: a) 0.475 %, b) 0.570 %, c) 0.713 %

strain amplitudes ($\Delta\varepsilon/2$). In **Figure 3**a, under a 0.475 % strain amplitude, the cyclic stress response behaviour is shown at 760 °C and 980 °C. At 760 °C, the cyclic stress response behaviour first exhibits a brief softening stage, then transitions to a hardening stage, where it remains

stable for an extended period in the middle of LCF, and then it experiences a sudden failure in the later stage. At 980 °C, the cyclic stress response shows a small difference, characterized by a progression of hardening, followed by softening, then a stable stage, and finally an abrupt failure.

On **Figures 3**b and **3c**, at strain amplitudes of 0.570 % and 0.713 %, the cyclic stress response curves exhibit similar trends at 760 °C and 980 °C. There are no obvious cyclic hardening and softening stages; the material basically maintains the cyclic stability throughout the LCF process. The difference in the curve is that the number of cycles before the alloy finally fails decreases as the temperature increases. This indicates that the higher the temperature, the lower is the LCF life of the alloy.

By comparing **Figures 3a** to **3c**, it can be seen that at low strain amplitudes, the difference in the temperature also creates a difference in the cyclic stress response behaviour, but at high strain amplitudes, the temperature difference has almost no impact on the alloy's cyclic stress response behaviour. Under three different strain amplitudes, the connection between the stress amplitude and fatigue life is also shown to be linear: the higher the stress amplitude, the shorter is the fatigue life. This is due to the fact that a higher strain amplitude will need a higher stress amplitude to create deformation, which will result in a shorter fatigue life.

3.3 Hysteresis loops and plastic strain energy

Under strain-controlled fatigue loading, materials usually enter a stable cyclic stage at around half of their fatigue life.[14] **Figure 4** shows hysteresis loops at around the half-life cycle for different strain amplitudes at two temperatures. Due to an asymmetric applied strain ratio (R = 0.05), the hysteresis loops of the DD419 alloy are asymmetric about the origin but symmetric about the strain axis during the half-life period.

At 760 °C, the shape of the hysteresis loops does not change significantly and approximates a straight line for all strain amplitudes. This suggests that the alloy's LCF process mainly involves elastic deformation, with very limited plastic deformation and damage. As the strain amplitude increases, the area of the hysteresis loops gradually expands, indicating increased plastic deformation and reduced fatigue life. At 980 °C, the area of the hysteresis loop obviously increases compared to 760 °C. Simultaneously, this area increases with the strain amplitude.

The area enclosed by hysteresis loops serves as a measure of the plastic strain energy value. Its physical meaning is that the larger the area of a hysteresis loop, the greater is the energy dissipation during plastic deformation, which makes the material more prone to fatigue damage and a lower life.[15] Generally, the value of plastic strain energy is obtained by integrating the area of the hysteresis loop. Previous studies revealed that the value

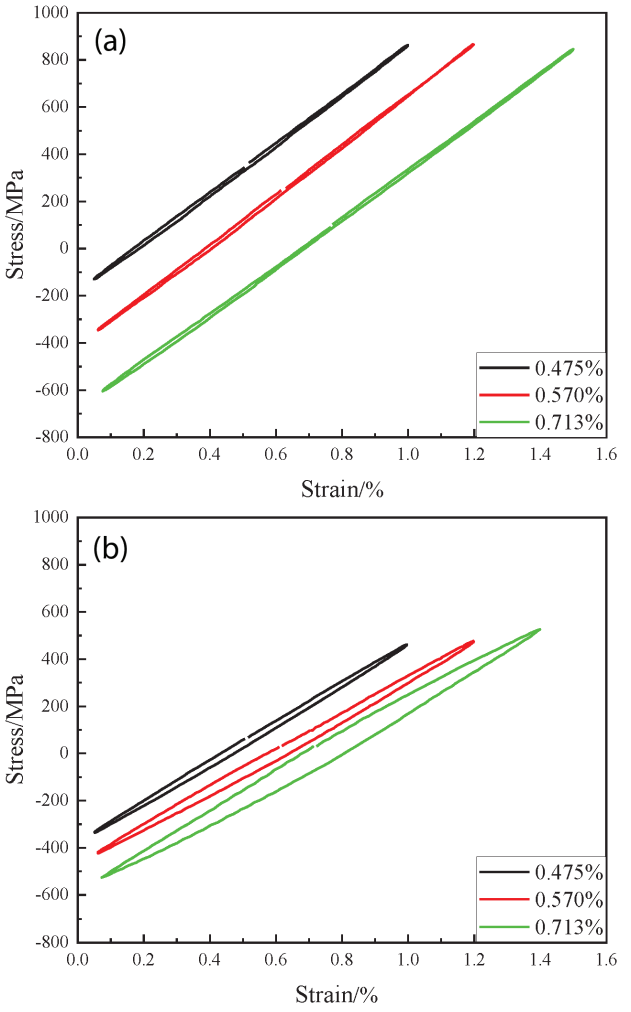

Figure 4: Hysteresis loops of alloys at different strain amplitudes: a) 760 °C, b) 980 °C

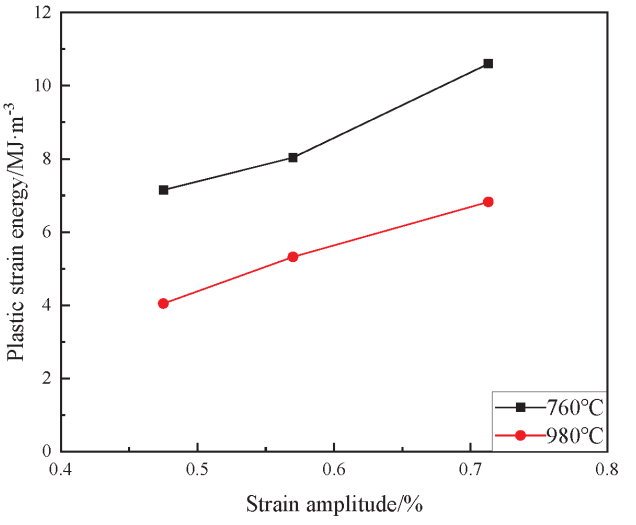

Figure 5: Relationship between strain amplitude and plastic strain energy of the alloy

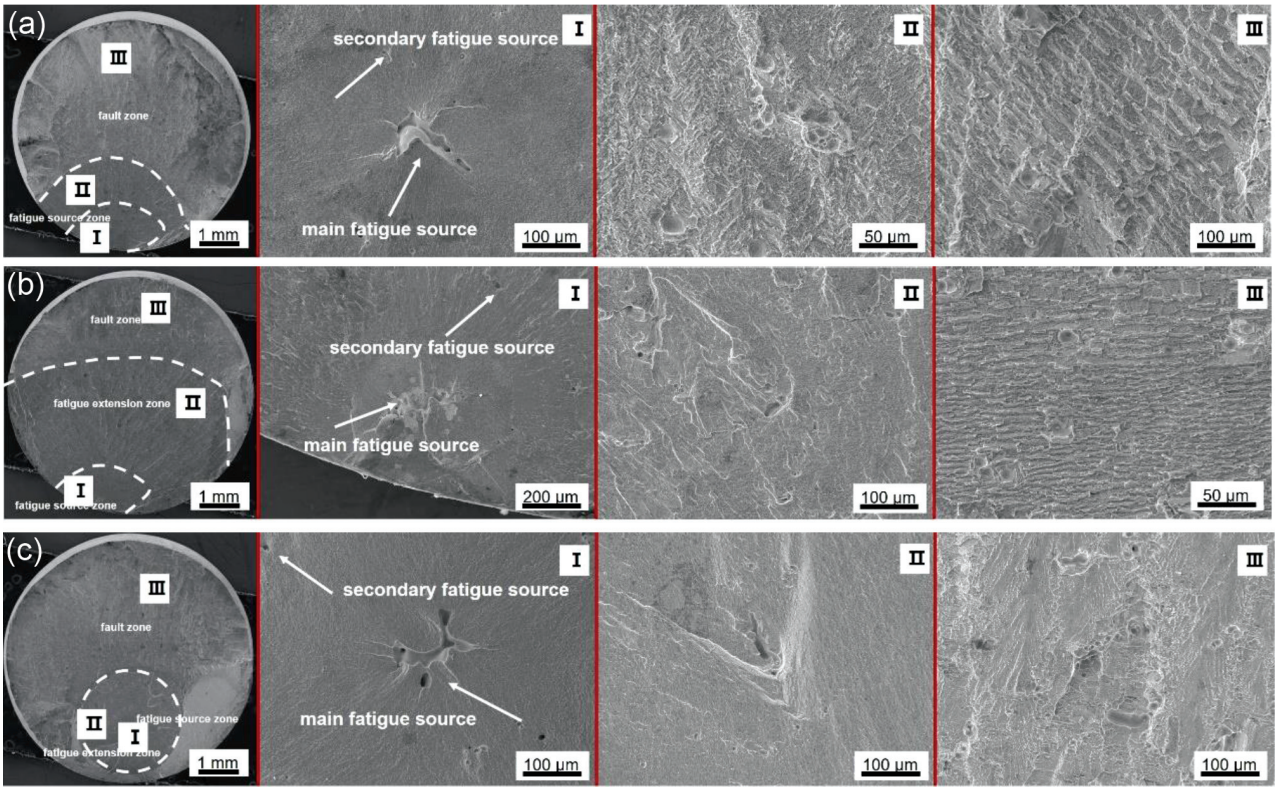

Figure 6: Fracture topography at 760 °C, a) 0.475%, b) 0.570%, c) 0.713%

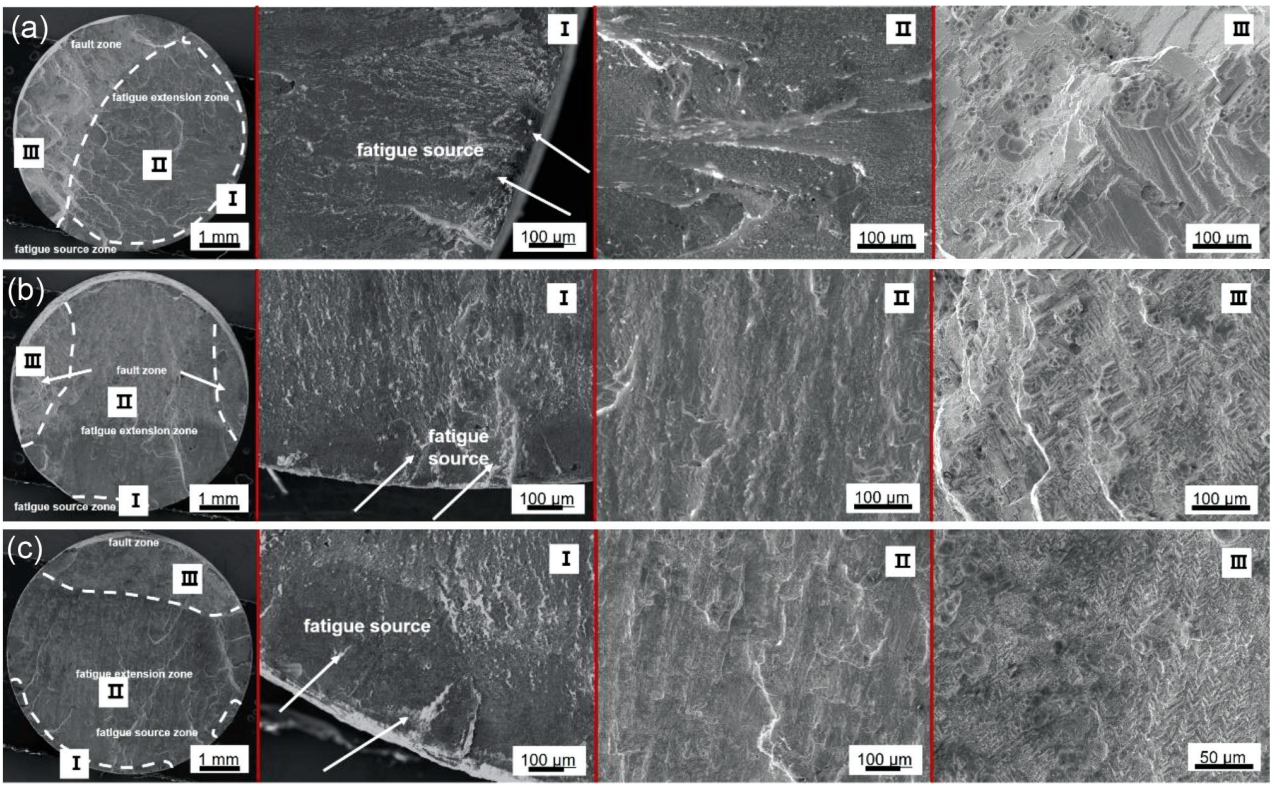

Figure 7: Fracture topography at 980 °C: a) 0.475%, b) 0.570%, c) 0.713%

of the plastic strain energy is primarily influenced by crystal orientation, as well as average stress and strain amplitude.[16]

Figure 5 illustrates the relationship between the strain amplitude and measured plastic strain energy. It is observed that the plastic strain energy increases with an increase in the strain amplitude at different temperatures. According to the principle of energy conservation, the energy expended in fracturing each sample remains constant. Therefore, a higher plastic strain energy consumed per cycle indicates a reduced number of cycles. This suggests that fatigue life diminishes with increasing strain amplitude, which is consistent with the findings of the strain-life curve.

3.4 Fracture behaviour

Fracture morphologies of specimens after the LCF fracture under different strain amplitudes and temperatures are shown in **Figures 6** and **7**. A typical fatigue fracture surface includes a fatigue source, fatigue extension zone, and transient fault zone.[17,18] Illustrations on the right show enlarged details of the three zones. As shown in **Figure 6**, at 760 °C the division between the zones is obvious. The cross-section of the fracture after fatigue still remains circular, which is typical of brittle fracture. There is no significant difference in the fatigue fracture morphology under different strain amplitudes. The main fatigue sources (aI, bI, and cI) all stem from surface defects (such as porosity and casting defects). Secondary fatigue sources can also be observed around the main fatigue sources, indicating multiple fatigue sources. This is because the slip system operated by the single-crystal superalloy at 760 °C is the octahedral slip system, and the slip can occur in different directions.[19]

After a fatigue source appears, the crack gradually expands and eventually forms an expansion zone. At this time, there are traces of metal slip and some torn edges in the expansion zone (aII, bII, and cII). Based on the microscopic expansion pattern, it can be inferred that the crack growth is of an open type. When the stress continues to increase, it leads to the eventual fracture of the alloy and the formation of a transient fault zone within the fracture. It is found that the macroscopic morphology of transient fault zones is rough, and microscopic cleavage steps are formed (aIII, bIII, and cIII). Therefore, the fracture of the alloy at 760 °C is a cleavage fracture.[20]

As shown in **Figure 7**, from a macro perspective, the fracture morphology at 980 °C is also composed of three parts, but the boundaries of each region are not clearly defined. The fracture shape after fatigue shows no obvious elongation or necking phenomenon, which is characteristic of typical brittle fractures. The crack propagation traces on **Figure 7** are more pronounced than those at 760 °C, and multiple crack sources can also be observed. From a microscopic perspective, fatigue cracks are initiated at the edge oxide of the sample (aI, bI, and cI) when the strain amplitudes are (0.475, 0.570, and 0.713) %. This occurs because the high temperature leads to the formation of a significant oxide layer on the alloy's surface. This, in turn, causes stress concentration on the surface, creating a source of fatigue that initiates cracking. There are also oxidation traces and metal slip traces in the fatigue extension zone (aII, bII, and cII), and the slip traces indicate the direction of crack propagation. The morphology of the instantaneous fracture zone is basically the same as that at 760 °C. The macroscopic appearance is relatively rough, and cleavage steps can be clearly observed under the microscope (aIII, bIII, and cIII). It is concluded that the fracture mechanism of the alloy at 980 °C is still a cleavage fracture.

In summary, under the same strain amplitude, changes in the temperature affect the location of fatigue source initiation but do not significantly impact other morphologies and fracture mechanisms. Similarly, at a constant temperature, variations in the strain amplitude do not alter the primary morphology of each region.

Figures 8 and **9** show transmission electron microscopy (TEM) images of the dislocation morphology after the LCF testing at a strain amplitude of 0.475 % and temperatures of 760 °C and 980 °C, respectively. The TEM morphology reveals that the main structures ob-

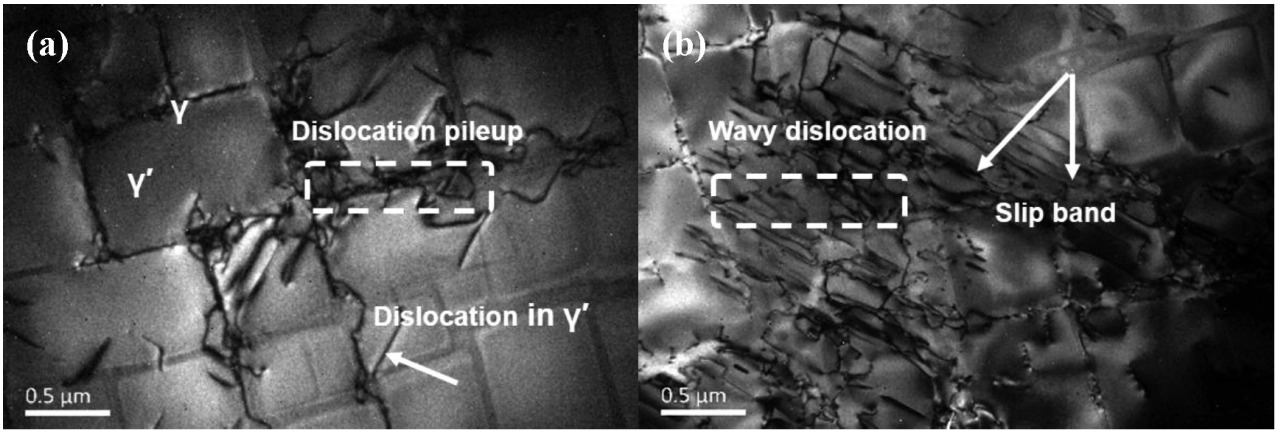

Figure 8: Microscopic morphology of dislocations at 760 °C: a) sample 1, b) sample 2

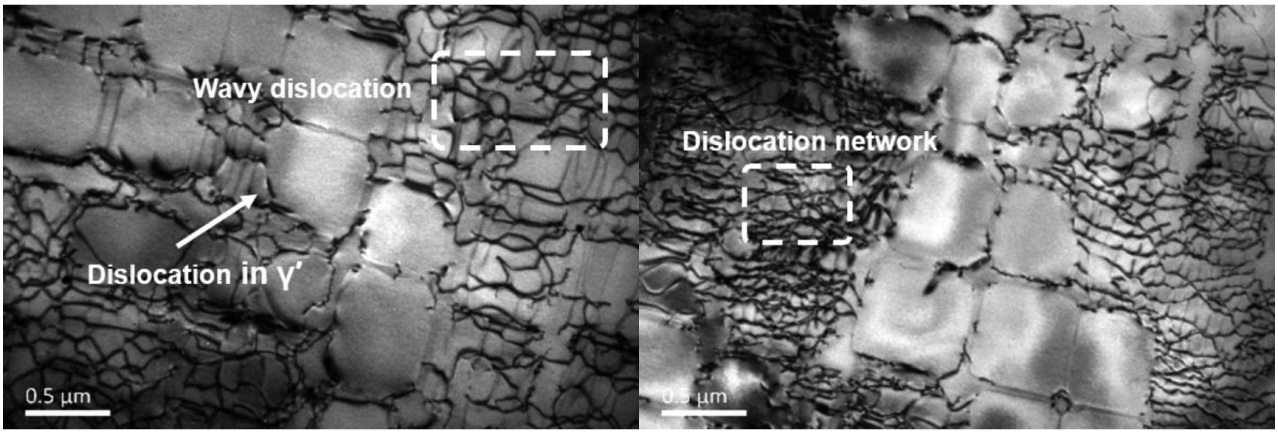

Figure 9: Microscopic morphology of dislocations at 980 °C: a) sample 1, b) sample 2

served after the LCF tests are the matrix γ phase and the strengthened γ' phase. Additionally, the transmission electron microscopy (TEM) morphology reveals highly uneven curved dislocation lines within the γ matrix channels of the DD419 alloy, which is consistent with the dislocation distribution characteristics observed in LCF fracture samples of other superalloys.[21]

At 760 °C, the γ' phases in **Figure 8a** are uniformly distributed with a distinct cubic shape. No angular dissolution or rafting phenomenon is observed, indicating that no creep damage occurred during the fracture of the sample. Some short dislocations are dispersed within the γ' phase, and their shearing of the γ' phase diminishes the strengthening effect of the γ' phase. It is also observed that a large number of screw dislocations continuously move into the matrix channel through cross slip and eventually plug up at the γ/γ' interface, contributing to the work hardening. Notably, in **Figure 8b**, a large number of slip bands composed of irregular dislocations and a small number of wavy dislocations can be clearly observed. The existence of wavy dislocations is a typical characteristic of wavy slip.[22] Therefore, the fracture mechanism of LCF at moderate temperatures exhibits characteristics of plane slip and wave slip, which is consistent with previous research findings.[23] In addition, a small number of stacking faults were found in the γ phase, which reduces the alloy's resistance to plastic deformation and leads to a rapid initiation of microcracks.

In **Figure 9**, the presence of angular dissolution or rafting of the γ' phase suggests that creep damage occurred during the fracture of the specimen at 980 °C. Additionally, short dislocations cut into the γ' phase (**Figure 9a**), and many high-density dislocations form a large number of dislocation networks that tangle around the γ/γ' interface (**Figure 9b**). According to previous studies,[24,25] this is the typical dislocation network structure in the primary stage of creep damage, and the density and morphology of dislocation networks play a crucial role in strengthening SX superalloys. At this point, due to the increase in the temperature, thermal activation becomes stronger, causing the stacking faults to disappear, leading to a change in the dislocation motion mode. The dislocations clustered at the γ/γ' interface continue to move around the γ' phase through climbing, and then proceed to advance through slippage or cross-slip mechanisms, resulting in a uniform distribution of dislocations. Therefore, the stress concentration in the γ phase is reduced, and the local hardening effect caused by dislocation entanglement is cancelled out. This demonstrates cyclic stability in the cyclic stress response curve (**Figure 3**).

Temperature plays a crucial role in the movement of dislocations and the formation of dislocation structures in nickel-based superalloys. **Figure 10** shows the effect of temperature on the microscopic deformation mechanism of the alloy.[26] As shown in **Figure 10**, the dislocation movement mode changes from planar slip to wave slip at 760 °C. Some of the screw dislocations move outward around the γ' phase in an arch shape through cross slip, while more dislocations accumulate at the γ/γ' interface. Finally, the accumulated dislocations will still pass through the γ' phase, leading to strain localization. When

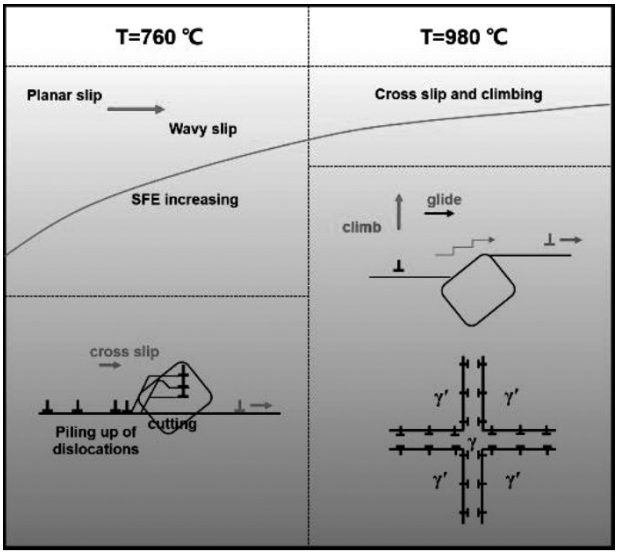

Figure 10: Effect of temperature on the microscopic deformation mechanism of the alloy

the temperature reaches 980 °C, the edge of the γ' phase dissolves significantly. As the stacking fault energy (SFE) increases, the stacking fault disappears, and the mismatch stress at the γ/γ' interface rises. This leads to the formation of a large number of dislocation networks due to the accumulated dislocations at the γ/γ' interface, increasing the difficulty of cutting the γ' phase. In addition, under the influence of thermal activation, the newly formed dislocations can move and traverse the γ' phase through climbing. They can then advance through glide or cross slip on the matrix channel {111} plane, ensuring a uniform distribution of dislocations.

4 CONCUSIONS

1) The LCF life of DD419 alloy is significantly influenced by temperature. Elastic deformation plays a crucial role in determining the LCF life of alloys at 760 °C and 980 °C. However, when compared to 760 °C, at 980 °C, the alloy shows increased plastic deformation, leading to reduced fatigue performance, shorter lifespan, and more severe damage.

2) The cyclic stress response behaviour of alloys at two different temperatures varies significantly. At low strain amplitudes, temperature differences can also lead to variations in the cyclic stress response behaviour of alloys. However, at high strain amplitudes, temperature differences have a minimal impact on the cyclic stress response behaviour of alloys. The hysteresis loop of alloys typically stabilizes near the half-life. As the strain amplitude increases, the plastic strain energy gradually rises, leading to a decrease in the fatigue life and performance.

3) At 760°C and 980°C, the fatigue fracture exhibits multiple fatigue sources, and the transient fracture zone displays cleavage steps, indicating a cleavage fracture. At 760 °C, fatigue source mainly initiates at surface defects. The fatigue source at 980 °C is mainly surface oxide.

4) At 760 °C, the alloy exhibits short dislocations and shearing of the γ' phase within slip bands, along with wavy dislocations near the γ/γ' interface. Hence, the LCF deformation mechanism of the alloy at 760 °C combines characteristics of both planar slip and wavy slip. At 980 °C, high-temperature creep damage mainly occurs in matrix dislocations and interface dislocations, with only a few dislocations passing through the γ' phase. The deformation mechanism mainly involves cross slip and climb around the γ' phase.

Acknowledgment

This research was funded in 2023 by the Liaoning Provincial Applied Basic Research Project (2023JH2/101300233), National Natural Science Foundation of China (No. 12375305), and Basic Research Projects of Higher Education Institutions in Liaoning Province (JYTZD20230004, JYTMS20230193).

5 REFERENCES

[1] L. Liu, J. Meng, J. L. Liu, T. Jin, X. D. Sun, H. F. Zhang, Effects of crystal orientations on the cyclic deformation behavior in the low cycle fatigue of a single crystal nickel-base superalloy, Materials & Design, 131 (**2017**), 441–449, doi:10.1016/j.matdes.2017.06.047

[2] Z. X. Shi, X. G. Wang, S. Z. Liu, J. R. Li, Low cycle fatigue properties and microstructure evolution at 760 °C of a single crystal superalloy, Progress in Natural Science: Materials International, 25 (**2015**), 78–83, doi:10.1016/j.pnsc.2015.01.009

[3] L. B. Yang, X. N. Ren, C. C. Ge, Q. Z. Yan, Status and development of powder metallurgy nickel-based disk superalloys, Int. J. Mater. Res, 110 (**2019**), 901–910, doi:10.3139/146.111820

[4] A. Shyam, W. W. Milligan, Effects of deformation behavior on fatigue fracture surface morphology in a nickel-based superalloy, Acta Mater., 52 (**2004**), 1503–1513, doi:10.1016/j.actamat.2003.11.032

[5] Y. L. Lu, L. J. Chen, G. Y. Wang, M. L. Benson, P. K. Liaw, S. A. Thompson, J. W. Blust, P. F. Browning, A. K. Bhattacharya, J. M. Aurrecoechea, D. L. Klarstrom, Hold time effects on low cycle fatigue behavior of HAYNES 230 superalloy at high temperatures, Materials Science & Engineering A, 409 (**2005**), 282–291, doi:10.1016/j.msea.2005.05.120

[6] M. Marchionni, G. A. Osinkolu, G. Onofrio, High temperature low cycle fatigue behaviour of UDIMET 720 Li superalloy, Int. J. Fatigue, 24 (**2002**), 1261–1267, doi:10.1016/s0142-1123(02)00043-9

[7] J. S. Wan, Z. F. Yue, A low-cycle fatigue life model of nickel-based single crystal superalloys under multiaxial stress state, Materials Science & Engineering A, 392 (**2005**), 145–149, doi:10.1016/j.msea.2004.09.069

[8] Z. D. Fan, D. Wang, L. H. Lou, Corporate Effects of Temperature and Strain Range on the Low Cycle Fatigue Life of a Single-Crystal Superalloy DD10, Acta Metall. Sin. (Engl. Lett.), 28 (**2015**), 152–158, doi:10.1007/s40195-014-0179-3

[9] Q. Q. Ding, H. B. Bei, X. Yao, X. B. Zhao, X. Wei, J. Wang, Z. Zhang, Temperature effects on deformation substructures and mechanisms of a Ni-based single crystal superalloy, Appl. Mater., 23 (**2021**), 1101061, doi:10.1016/j.apmt.2021.101061

[10] L. J. Chen, D. Wang, X. Che, F. Li, Low-cycle fatigue behavior of permanent mold cast and die-cast Al-Si-Cu-Mg alloys, China Foundry, 9 (**2012**), 39–429, doi:CNKI:SUN:ZZAF.0.2012-01-011

[11] X. F. Ma, H. J. Shi, J. L. Gu, Z. X. Wang, H. Harders, T. Malow, Temperature effect on low-cycle fatigue behavior of nickel-based single crystalline superalloy, Acta Mechanica Solida Sinica, 21 (**2008**), 289–297, doi:10.1007/s10338-008-0833-2

[12] M. H. Hirschberg, S. S. Manson, Fatigue behavior in strain cycling in the low- and intermediate-cycle range, Fatigue – An Interdisciplinary approach, 33 (**1964**), 133–173

[13] J. Xie, D. L. Shu, G. C. Hou, J. J. Yu, Y. Z. Zhou, X. F. Sun, Low-cycle fatigue behavior of K416B Ni-based superalloy at 650 °C, Journal of Central South University, 9 (**2021**), 2628–2635, doi:10.1007/s11771-021-4797-4

[14] L. Zhang, L. G. Zhao, A. Roya, V. Silberschmidta, G. Mccolvinb, Low-cycle fatigue of single crystal nickel-based superalloy mechanical testing and TEM characterization, Mater. Sci. Eng, A, 744 (**2019**), 538–547, doi:10.1016/j.msea.2018.12.084

[15] D. Kujawski, F. Ellyin, A cumulative damage theory for fatigue crack initiation and propagation, Int. J. Fatigue, 6 (**1984**), 83–88, doi:10.1016/0142-1123(84)90017-3

[16] F. Ellyin, Effect of Tensile-Mean-Strain on Plastic Strain Energy and Cyclic Response, J. Eng. Mater. Technol., 107 (**1985**), 119, doi:10.1115/1.3225786

[17] L. Shui, P. Liu, Low-cycle fatigue behavior of a nickel based single crystal superalloy at high temperature, Rare Metal Materials and Engineering, 44 (**2015**), 288–292, doi:10.1016/S1875-5372(15)30021-7

[18] P. F. Wang, X. B. Zhao, Q. Z Yue, W. S. Xia, Q. Q. Ding, H. B. Bei, Y. F. Gu, X. Wei, Z. Zhang, Deformation mechanisms of low cycle fatigue of a fourth generation Ni-based single crystal superalloy, J.

Mater. Res. Technol., 24 (**2023**), 2053–2063, doi:10.1016/j.jmrt.2023.03.148

[19] H. Lu, J. Wang, Y. Lian, Z. Wen, T. Liu, Z. Yue, Effect of orientation deviation on random vibration fatigue behavior of nickel based single crystal superalloy, Int. J. Fatigue, 177 (**2023**), 107930, doi:10.1016/j.ijfatigue.2023.107930

[20] Z. Shi, S. Liu, X. Yue, J. Li, Anisotropic Creep Behavior of DD15 Single Crystal Superalloy, Rare Metal Materials and Engineering, 51 (**2022**), 3542–3546, doi:10.12442/j.issn.1002-185X.20220197

[21] Y. Y. Guo, Y. S. Zhao, J. Zhang, Y. F. Liu, Y. S. Luo, J. B. Sha, Effect of Strain Amplitude on Cyclic Deformation Behavior of Nickel-Based Single Crystal Superalloy DD11 in Low Cycle Fatigue, Rare Metal Materials and Engineering, 48 (**2019**), 366–374

[22] P. F. Wang, X. B. Zhao, Q. Z. Yue, W. S. Xia, Q. Q. Ding, H. B. Bei, Y. F. Gu, Y. F. Zhang, Z. Zhang, Influence of Strain Amplitude on Low-Cycle Fatigue Behaviors of a Fourth-Generation Ni-Based Single-Crystal Superalloy at 980°C, Crystals, 13 (**2023**), 686, doi:10.3390/cryst13040686

[23] L. Liu, J. Meng, J. L. Liu, H. F. Zhang, X. D. Sun, Y. Z. Zhou, Investigation on low cycle fatigue behaviors of the [001] and [011] oriental single crystal superalloy at 760 °C, Mater. Sci. Eng. A, 734 (**2018**), 1–6, doi:10.1016/j.msea.2018.07.078

[24] J. Zhang, Y. Y. Guo, M. Zhang, Z. Y. Yang, Y. S. Luo, Low-Cycle Fatigue and Creep-Fatigue Behaviors of a Second-Generation Nickel-Based Single-Crystal Superalloy at 760 °C, Acta Metall. Sin. (Engl. Lett.), 33 (**2020**), 1423–1432, doi:10.1007/s40195-020-01056-6

[25] X. G. Wang, J. L. Liu, T. Jin, X. F. Sun, Y. Z. Zhou, Z. Q. Hu, J. H. Do, B. G. Choi, I. S. Kim, C. Y. Jo, Deformation mechanisms of a nickel-based single-crystal superalloy during low-cycle fatigue at different temperatures, Scr. Mater., 99 (**2015**), 57–60, doi:10.1016/j.scriptamat.2014.11.026

[26] P. Li, Q. Q. Li, T. Jin, Y. Z. Zhou, J. G. Li, X. F. Sun, Z. F. Zhang, Comparison of low-cycle fatigue behaviors between two nickel-based single-crystal superalloys, Int. J. Fatigue, 63 (**2014**), 137–144, doi:10.1016/j.ijfatigue.2014.01.018